

Article

Characterizing Land Surface Temperature (LST) through Remote Sensing Data for Small-Scale Urban Development Projects in the Gulf Cooperation Council (GCC)

Maram Ahmed ¹, Mohammed A. Aloshan ^{2,*}, Wisam Mohammed ³, Essam Mesbah ⁴, Naser A. Alsaleh ⁵ and Islam Elghonaimy ⁶

¹ College of Science, University of Bahrain, Zallaq 1054, Bahrain; 20151531@stu.uob.edu.bh

² Department of Architectural Engineering, Imam Mohammad Ibn Saud Islamic University (IMSIU), Riyadh 12211, Saudi Arabia

³ Landscape Architecture Department, College of Architecture and Planning, Imam Abdulrahman Bin Faisal University, Dammam 32210, Saudi Arabia; wemahmoud@iau.edu.sa

⁴ Department of Architectural Engineering, College of Engineering, University of Jeddah, Jeddah 21589, Saudi Arabia; emosbah@uj.edu.sa

⁵ Department of Industrial Engineering, Imam Mohammad Ibn Saud Islamic University (IMSIU), Riyadh 12211, Saudi Arabia; naalsaleh@imamu.edu.sa

⁶ Department of Architecture and Interior Design, The College of Engineering, University of Bahrain, Zallaq 1054, Bahrain; eelghonaimy@uob.edu.bh

* Correspondence: mamoshan@imamu.edu.sa; Tel.: +966-54-249-9915

Abstract: In the context of global climate change, there is a projected increase in land surface temperature (LST) worldwide, amplifying its impacts. This poses a particular concern for countries with hot climates, including the Kingdom of Bahrain as an example for the Gulf Cooperation Council countries (GCC), which are countries with a hot climate. With a surge in population growth, there is a heightened demand for land to accommodate additional residential developments, creating an opportunity to investigate the influence of land use changes on LST variations. To achieve this goal, a residential development project spanning from 2013 to 2023 was undertaken. Landsat 8 OLI/TIRS remote sensing datasets were selected for four climate seasons, each set comprising images before and after development. The analysis involved extracting the LST, Normalized Difference Vegetation Index (NDVI), and Normalized Difference Built-Up Index (NDBI) on various dates, followed by correlation and regression analyses to explore their interrelationships. The results revealed a significant increase in the mean LST during spring and autumn post-development. A consistent positive association between the LST and NDBI was observed across all seasons, strengthening after development completion. Conversely, there was a pre-development negative correlation between the LST and NDVI, shifting to a positive relationship post-development. These findings empirically support the idea that small-scale residential developments contribute to notable LST increases, primarily due to expanded impervious surfaces. These insights have the potential to inform localized adaptation strategies for small-scale residential development projects, crucial for managing the impacts of rising land surface temperatures.

Keywords: Bahrain; sustainability environmental quality; climate change adaptation; remote sensing; urban heat islands (UHIs); social housing project; governmental housing



Citation: Ahmed, M.; Aloshan, M.A.; Mohammed, W.; Mesbah, E.; Alsaleh, N.A.; Elghonaimy, I. Characterizing Land Surface Temperature (LST) through Remote Sensing Data for Small-Scale Urban Development Projects in the Gulf Cooperation Council (GCC). *Sustainability* **2024**, *16*, 3873. <https://doi.org/10.3390/su16093873>

Academic Editor: Alejandro Javier Rescia Perazzo

Received: 23 February 2024

Revised: 30 March 2024

Accepted: 28 April 2024

Published: 6 May 2024



Copyright: © 2024 by the authors. Licensee MDPI, Basel, Switzerland. This article is an open access article distributed under the terms and conditions of the Creative Commons Attribution (CC BY) license (<https://creativecommons.org/licenses/by/4.0/>).

1. Introduction

The urbanization process has resulted in noticeable alterations to the landscape, causing a decline in environmental conditions that negatively impact the overall quality of life. Urbanization contributes to increased air [1] and water pollution [2]. The alterations in landscape and human utilization profoundly impact the energy transfer between the Earth's surface and the atmosphere, resulting in an elevation in urban ambient temperature

that diverges from the temperatures seen in surrounding non-urbanized regions [3]. In urban areas, heat waves predominantly manifest in heat islands as a result of the elevated surface temperature concentration [4,5]. The rise in impervious surfaces such as roads and buildings exacerbate issues like the urban heat island effect and flooding, altering local climates and water cycles [1]. The uncomfortable conditions experienced by ecosystems can be attributable to times of extremely high temperatures [6]. The harsh impact of these heat waves has the potential to exacerbate health issues and potentially result in mortality [7]. In regions characterized by hot and arid climatic conditions, the confluence of weather patterns and heatwaves exerts a significant influence on the well-being of the local populace [8,9]. The urban thermal environment is a significant concern inside metropolitan areas, necessitating urban planning efforts that prioritize the development of policies aimed at establishing optimal living circumstances for residents [10].

Several studies have contributed to understanding the impact of urbanization on thermal and microclimate conditions. Yang et al. [2] conducted a comprehensive meta-analysis of urban microclimate research with an emphasis on the thermal environment and the methods of evaluating related phenomena, including traditional methods and emerging methods such as artificial intelligence or data-driven models. In their study, Das et al. [1] investigated the dynamics of landscape patterns and the impact of composition and configuration on the thermal environment of urban agglomeration. The researchers employed a mixed-methods approach, combining geospatial approaches, spatial metrics, and descriptive and inferential statistics to assess the impacts of urban composition and configuration within an urbanized area in India. Their findings revealed that the spatial composition and configuration of the impervious surface, green spaces, and blue spaces must be considered in landscape planning and design framework to make the city more livable [1].

In the Gulf Cooperation Council in general and Bahrain in particular, according to several studies about accruing urban heat islands (UHIs) in its cities due to urbanization projects, there are concerns about implementing residential projects that deteriorate the urban quality. In other words, there needs to be more understanding of the environmental impacts of such residential projects in the urban context. In other words, these projects have a shortage of implementing sustainability in their plans. Therefore, the main aim of this study was to investigate the influence of land use changes on LST variations in a small-scale urban landscape, putting the UHIs under the spotlight to enhance environmental construction practices in the region. Therefore, the research proposed three hypotheses: the first is that the NDVI has a substantial impact on the LST in the study area, the second is that the NDBI has a significant impact on the LST, and the third is both the NDVI and NDBI variables have a significant impact on the LST.

Remote sensing provides an effective tool to evaluate large-scale urban agglomerations, as examined in China [3], India [4], Europe [5,6], Australia [7], and other parts of world. For example, Pan et al. [3] conducted a comparative analysis of land surface temperature (LST) and the urban heat islands over three different urban agglomerations in China, emphasizing the potentials of using low spatial resolution remote sensing MODIS data for evaluating thermal settings over a large area. Several studies have investigated using remote sensing data for studying land surface temperature and related phenomena on a mesoscale. For example, Wu et al. [8] investigated the spatiotemporal characteristics and influencing factors of LST in the long term in a city-scale urban area using Landsat 8 datasets. Their insights provide valuable guidance for policymakers, urban planners, and environmental researchers to formulate evidence-based strategies to achieve a resilient, livable urban future. However, few studies have examined the land surface temperature, urban heat islands, and other urban microclimatic thermal phenomena on a small scale. For example, Naughton and McDonald [9] explored the thermal settings and land surface temperature in two locations, highlighting the role of using drone thermal imagery. Their findings elucidate factors that contribute to land surface temperature variability in a small-

scale urban environment, which can be applied to develop better temperature mitigation practices to protect human and environmental health [9].

In several nations, due to rapid urbanization in recent years, some development projects and unplanned and inefficient energy studies use strategies have led to increasingly severe alterations in the land surface temperature (LST) in urban areas. Several studies have indicated that the Gulf Cooperation Council (GCC) countries, namely the United Arab Emirates, Bahrain, Kuwait, Oman, Qatar, and Saudi Arabia, are expected to undergo significant urban expansion in the near future [11]. The urbanization rate in each of these countries has exceeded 80% over the past decade [12]. The expansion of metropolitan areas typically leads to a rapid growth of impervious surfaces, which, in turn, amplifies the rise in LST [13]. Although much focus has been given to the urban dynamics of major metropolitan areas in the area, middle-sized urban agglomerations and cities have not been thoroughly examined. Bahrain is a very typical example for such these urban agglomerations, which is located on an island in the central region of the Gulf area. As the main entry point to the region and an agglomeration with a population of one million, it has experienced rapid urbanization. Although there have been a few studies on urbanization in Bahrain, the correlation between LST and urbanization has not been investigated. Several researchers have studied the association between LST and land use and land cover in relation to climate change, urban planning, soil ecology, and vegetation health. Therefore, this study aimed to study the correlation between LST and the process of urbanization in the typical Gulf urban area of Bahrain. The current population of Bahrain in 2024 is 1,498,712, a 0.89% increase from 2023. The population of Bahrain in 2023 was 1,485,509, a 0.9% increase from 2022. The population of Bahrain in 2022 was 1,472,233, a 0.61% increase from 2021. The population of Bahrain in 2021 was 1,463,265, a 0.96% decline from 2020 [14]. Figure 1 elucidates the annual population growth from the beginning of the 1950s until 2024.

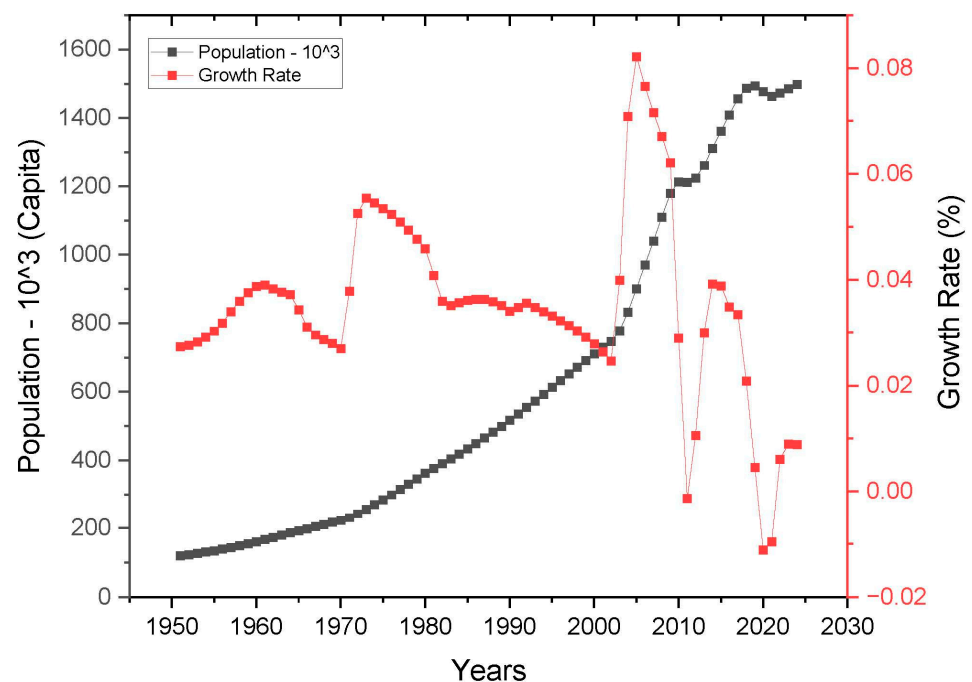


Figure 1. Population in Bahrain [15].

Due to the rising population in Bahrain, there is a growing need for developed land in the country. To mitigate the adverse environmental impacts of urban expansion, the Bahraini government has implemented a strategy of developing residential projects of various sizes to guarantee the availability of ecofriendly and high-quality housing. This phenomenon is a prevailing tendency throughout all GCC nations. It should be noted that sustainability is a broad frame that includes human beings' technical, environmental, cul-

tural, economic, and social sustainability. Understanding the significance of sustainability and achieving sustainable development for humanity, the research strives to support the Sustainable Development 2030 Agenda adopted by the United Nations and its implementation in the GCC. Therefore, one of the significant governmental objectives for doing such projects in the GCC is to guarantee sustainable projects. This phenomenon is a prevailing tendency throughout all GCC nations.

Consequently, within this frame, the topic at hand is whether the ongoing residential projects are ecologically sustainable and ensure quality of life. When evaluating sustainability and quality of life in a location with intense heat and humidity, as the countries in the GCC, it is crucial to consider human thermal comfort, which will positively impact the daily life of the residents and their social interaction within the urban context. In addition to improving their performance and ability to work hard in their daily jobs, in the same context, it will enhance the residents' overall performance and economics. This comfort is influenced by the land surface temperature.

The measurement of land surface temperature (LST) serves as a reliable indication for assessing the energy equilibrium at the Earth's surface. It is considered a fundamental parameter in the study of land–surface dynamics, both at the regional and global level. Several researchers have demonstrated the integration of surface–atmosphere interactions and energy fluxes between the atmosphere and the ground [16–18]. The term “land surface temperature (LST)” is commonly used to describe the temperature of the Earth's surface's skin layer. It encompasses the soil surface temperature for areas without vegetation cover and the canopy surface temperature for regions with extensive vegetation. The determination of the LST for urban areas is influenced by the temperatures of the vegetation canopy, vegetation body, and soil surface [19,20]. The LST is influenced by the Earth's surface effective radiating temperature, which governs the exchange of heat and water between the surface and the atmosphere [17,18]. It is a crucial parameter that governs several physical, chemical, and biological processes occurring on Earth. It holds significant importance in the investigation of the urban climate, as highlighted by several researchers [21,22]. The LST exhibits variability in accordance with the surface energy balance and plays a role in regulating the air temperature of the lower levels of the urban atmosphere. It holds a significant position in the energy balance of the surface and influences the energy exchanges that impact the comfort levels of urban residents [16].

Remote sensing techniques have proven to be effective in estimating the LST in urban ecosystems, as demonstrated by several researchers [23–25]. The use of moderate resolution multispectral satellite products, such as the Landsat 4–5 Thematic Mapper (TM), Landsat 7 Enhanced Thematic Mapper (ETM+), the Advanced Spaceborne Thermal Emission and Reflection Radiometer (ASTER), and Landsat 8–9 Thermal Infrared Sensor (TIRS), has been employed in various studies to estimate the spatiotemporal land surface temperature (LST) [26–28]. Prior studies have indicated that the thermal attributes and spatial arrangement linked to the LST are influenced by the composition and configuration of land use and land cover [29,30]. Several researchers have reported that the variation in LSTs across urban areas is primarily influenced by vegetation conditions, impervious surfaces, and soil functions [31,32]. Hence, it can be inferred that the biophysical components mentioned in different studies are influenced by seasonal fluctuations and are hypothesized to exhibit nonlinearity in relation to the LST [20,33]. In contrast, additional research has provided further support for the proposition that socioeconomic factors, such as income, population characteristics, and educational level, exert an influence on the LST [34,35].

2. Materials and Methods

2.1. Study Area

The Kingdom of Bahrain is located in the Arabian Gulf on the east coast of the peninsula. It is an island country with a limited land area; its geographical location and characteristics are similar to other regions on the east coast of the Arabian Peninsula. Given the similarities in geographical factors and proximity to other regions on the east coast of

the Arabian Peninsula, the results of a study conducted in Bahrain can provide insights and knowledge that may apply to different regions in the area, especially the eastern coast of Saudi Arabia, State of Qatar, and UAE.

Elagib, N. A. and Abdu A. S. [36] mentioned that, due to the significant and fluctuating changes in climatic conditions, this area has been classified as a desert or hyperacid. The highest temperature is recorded in April, reaching 8.8 °C, while the lowest temperature of 5.9 °C is observed in November. The average monthly rainfall in Bahrain can reach a maximum of 16.2 mm in January, while the yearly precipitation is 76.0 mm. There is a distinct interruption in the rainfall pattern throughout the year, with a continuous absence of rainfall for four consecutive months from June to September [36]. Due to its population density of around 2000 individuals per square kilometer and its restricted land area as an island state, Bahrain experiences a significant demand for housing.

The Al Ramila suburb is located in the “A’ali” District in Northern Governorate, Bahrain. Its coordinates are 26°09’07” N 50°31’32” E. A’ali is famous for its ancient burial mounds, especially several huge burial mounds in the city center. It is surrounded by new phases of governmental residential projects to the east and north of it, with a storage zone on the west side and the existing residential district to the south.

A’ali is also renowned for its traditional handcrafted pottery, which can be seen and bought from different potters and boutiques throughout the town. It should be noted that most of the Al Ramila suburbs were dumping areas for demolished construction projects in Bahrain. It was used for a long time until the governorate decided to construct several residential projects there and stopped using it as a dumping area. The study area had a shortage of vegetation for a long time due to its function as a construction dumping area, which negatively affected its land characteristics.

The Al Ramila suburb is one of several projects being created in Bahrain to meet the demand for housing. The Al Ramli suburb area covers 107.216 hectares. Figure 2a illustrates the exact bounds of the Al Ramila suburb, while Figure 2b,c depict the precise micro and macro locations, respectively. The suburb is extended from 50°30’26.47” E to 50°31’15.00” E and from 26°10’03.26” N to 26°10’46.29” N.

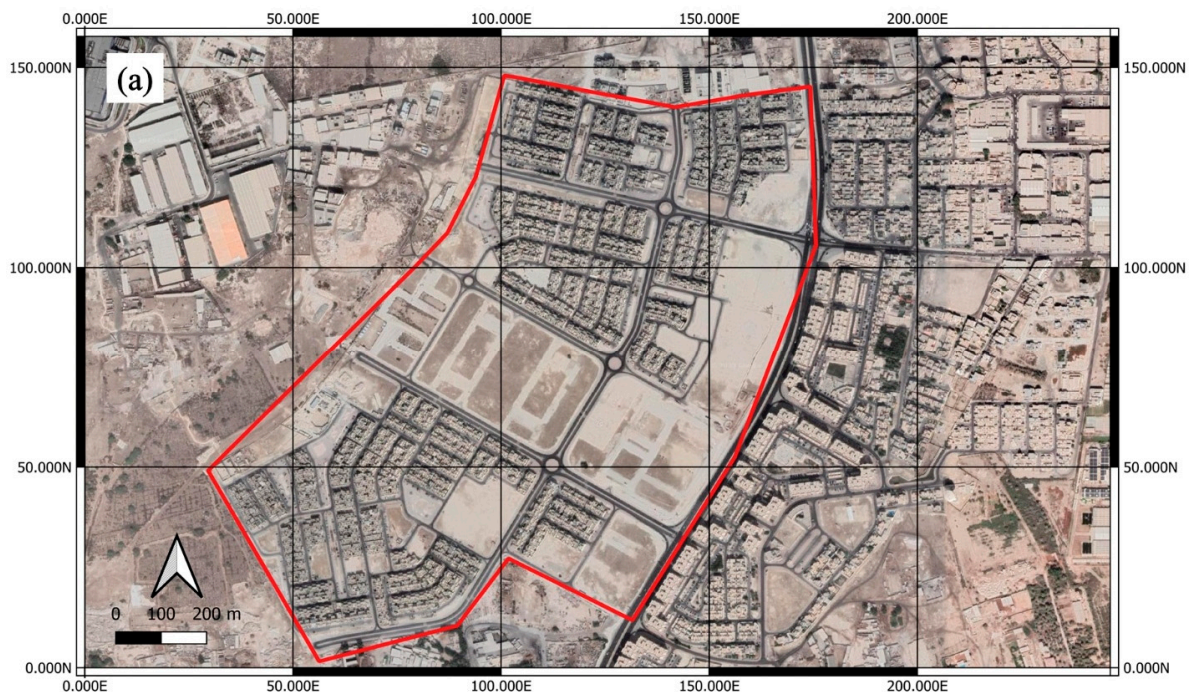


Figure 2. Cont.

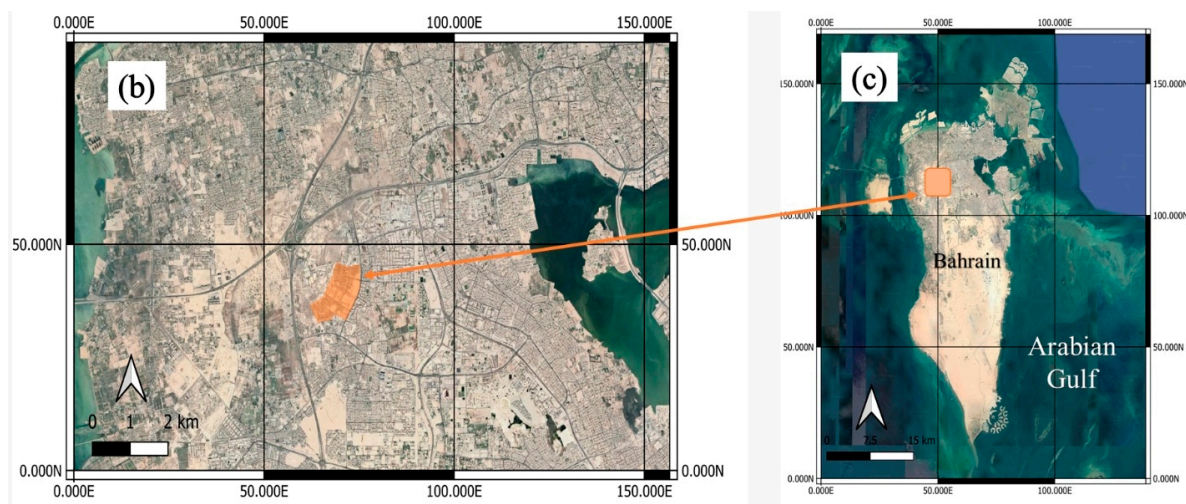


Figure 2. Location of the study area. (a). location borders of the designated study area, (b). Micro location, (c). macro location (based on Google maps, edited by the researchers).

The Al Ramli suburb offers its people a sustainable and self-sufficient lifestyle, with a total of 4501 dwellings and apartment units available. The project will distribute almost 65% of its resources to residential areas, 14.3% to key roadways, 5.67% to educational buildings, 1.74% to a public garden, 8.3% to social services, 1.85% to public amenities, and 2.20% to other objectives.

2.2. Data

The Landsat program is managed by the United States Geological Survey (USGS). Landsat 8 OLI/TIRS images consist of 11 bands, with bands 10 and 11 being designated as thermal bands. The Landsat 8 images possess a spatial resolution of 30 m, a radiometric resolution of 12 bits, and a temporal resolution of 16 days. The thermal bands have a spatial resolution of 100 m, which is then resampled to 30 m for distribution [37]. Four sets of Landsat 8 images were obtained from the USGS Earth Explorer portal (<https://earthexplorer.usgs.gov/>) (accessed on 14 February 2023). Each set consists of two images: one taken in 2013/2014 (before the development of the Al Ramli District) and another taken in 2022/2023 (after the development); see Table 1. These images were captured for Path 163 and Row 42 during the daytime. In this study, we utilized three spectral bands from the Landsat 8 satellite data (namely, Band 4 for Red, Band 5 for Near-Infrared, and Band 6 for Shortwave Infrared) to calculate the spectral indices. Band 10 (TIR10) and Band 11 (TIR11) are both intended for measuring the land surface temperature. However, Band 10 is preferable for a quantitative analysis due to its lower contamination from stray light compared to Band 11. The study area was clipped from all images for the purpose of the study.

Table 1. Dates of the obtained Landsat 8 OLI/TIRS images.

Season	Before Development	After Development
Spring	27 March 2013	19 April 2022
Summer	7 July 2013	16 July 2022
Autumn	27 October 2013	15 October 2022
Winter	15 January 2014	8 January 2023

The researchers conducted four visits to the study area on 10 January 2022, 1 April 2022, 3 July 2022, and 28 September 2022, with the objective of studying the land use and land cover in the study area. They recorded their visits using photos, as seen in Figure 3.



Figure 3. A photo of the study area (source: author).

3. Methodology

This study employs remote sensing data to extract the land surface temperature and environmental spectral indices, including the Normalized Difference Vegetation Index (NDVI) which is the numerical indicator for evaluating the health and density of vegetation [30], and the Normalized Difference Built-Up Index (NDBI) which is the index of built-up or areas [35]. These indices are used to assess thermal and environmental conditions for small- and medium-scale projects. This approach was applied to every Landsat 8 image used in this study. The borders of the study region were used to clip all Landsat images. The images were presented in the form of integer numbers known as digital numbers (DNs). The conversion process specified in the Landsat 8 Data User Handbook [38] was used to convert the images to top-of-atmosphere (TOA) reflectance. As per this method and using Equation (1), the Landsat images were transformed from DN to at-sensor radiance using the following equation:

$$L_{\lambda} = M_L \cdot Q_{cal} + A_L \quad (1)$$

where L_{λ} is the spectral at-sensor radiance, M_L is the radiance multiplicative scaling factor for the band L, Q_{cal} is the quantized calibrated pixel value, and A_L is the radiance additive scaling factor for the band L.

The conversion from at-sensor radiance to top-of-atmosphere reflectance was achieved using Equation (2) as shown below:

$$\rho_{\lambda} = \frac{\pi \cdot L_{\lambda} \cdot d^2}{ESUN_{\lambda} \cdot \cos \theta_s} \quad (2)$$

where ρ_{λ} is the unitless top-of-atmosphere (TOA) reflectance, d is the Earth–Sun distance measured in astronomical units, $ESUN_{\lambda}$ is the mean solar exoatmospheric irradiance, and θ_s is the solar zenith angle.

The at-surface reflectance was derived using the dark object subtraction (DOS) method applied to the top-of-atmosphere (TOA) reflectance to eliminate atmospheric interference. Dark object subtraction (DOS) is a straightforward and empirical technique used to remove atmospheric effects in remote sensing data. It operates under the assumption that the reflectance of dark objects contains a significant portion of atmospheric scattering. The DOS algorithm scans each band to identify the pixel with the lowest intensity and subsequently eliminates unwanted atmospheric distortions by removing this value from every pixel in the band [39].

This study utilized the NDVI as its primary index. The utilization of the NDVI was initially employed for evaluating the existence of vegetation, a purpose that has been substantiated in previous research [40,41]. The NDVI is traditionally calculated by taking the ratio of at the surface red reflectance to near-infrared reflectance as exposed in Equation (3):

$$NDVI = \frac{NIR - R}{NIR + R} \quad (3)$$

The at-surface reflectance in the near-infrared (NIR) and visible red (R) can be measured using Band 5 and Band 4 of Landsat 8 OLI. The index spans a range from 0 to 1, with higher values indicating higher vegetation cover.

The index employed herein is organized into five distinct classifications to delineate various land cover types. The classifications are defined as follows:

- i. Class 0: Representative of areas characterized by clouds and water.
- ii. Class 0–0.1: Encompassing terrains featuring rock and bare soil.
- iii. Class 0.1–0.3: Designating regions identified as barren areas.
- iv. Class 0.3–0.7: Inclusive of landscapes characterized by shrubs, crops, and grassland.
- v. Class > 0.7: Indicative of areas exhibiting a prevalence of dense vegetation.

This classification system serves as a meticulous framework, enabling a comprehensive assessment of land cover types based on the specified index intervals.

The Normalized Difference Built-up Index (NDBI) is a spectral indicator designed for studying built-up areas. The calculation involves determining the ratio between the shortwave infrared (SWIR) and near-infrared (NIR) wavelengths, as shown in Equation (4). Areas with a dense build-up exhibit a greater reflection of shortwave-infrared (SWIR) radiation, whereas areas with less dense build-up display a lower level of reflectance in the near-infrared (NIR) spectrum [40]. The calculation of the NDBI was performed using the following equation [41,42]:

$$NDBI = \frac{SWIR - NIR}{SWIR + NIR} \quad (4)$$

The NDVI, which stands for the Normalized Difference Vegetation Index, is the predominant and extensively employed metric for vegetation extraction. As mentioned in the Methodology, Equations (3) and (4) defined how the Normalized Difference Vegetation Index (NDVI) and Normalized Difference Built-Up Index (NDBI) are extracted from Landsat data.

In Landsat 8, Band 5 and Band 6 represent near-infrared and shortwave infrared, and the NDBI was obtained using at-surface reflectance. The index ranged from -1 to 1 , with a higher value signifying an increase in built-up cover.

The index employed in this investigation has been partitioned into four distinct classifications, each associated with specific numerical ranges. These classifications are defined as follows:

- i. Class ≤ -0.05 : Signifying non-settlement areas.
- ii. Class -0.05 – -0.01 : Representing regions characterized by low built area density.
- iii. Class -0.01 – 0.049 : Indicative of areas with medium built area density.
- iv. Class > 0.49 : Denoting regions featuring high built area density.

To obtain the land surface temperature (LST) from Landsat 8 Band 10, the band was transformed into spectral at-sensor radiance using a radiative transfer equation and the radiative transfer theory-based method [43] (Equation (1)). This radiance was then utilized to derive the brightness temperature T_B in Kelvin using Equation (5), as shown below:

$$T_B = \frac{k_2}{\ln\left(\frac{k_1}{L_\lambda} + 1\right)} \quad (5)$$

where k_1 and k_2 are calibration constants that equal 774.89 and 1321.08, respectively, for Landsat 8 Band 10.

The surface emissivity (ε) was determined with the use of the NDVI thresholds approach [44,45]. The fractional vegetation (F_v), which is defined as the proportion of the vertical projected area occupied by green vegetation to the total ground area, expressed as a percentage is revealed in Equation (6) [46], was calculated based on the Normalized Difference Vegetation Index (NDVI) using the following equation [47]:

$$F_v = \left[\frac{NDVI - NDVI_{min}}{NDVI_{max} - NDVI_{min}} \right]^2 \quad (6)$$

where $NDVI_{min}$ refers to the minimum value of the NDVI at which pixels are classified as bare soil, and $NDVI_{max}$ represents the maximum value of the NDVI at which pixels are classified as healthy vegetation.

Land surface emissivity (ε_λ) is the measure of how effectively a surface releases heat radiation. ε_λ is a quantitative assessment of a surface's ability to emit heat by infrared radiation relative to a perfect emitter called a blackbody. In theory, the ε_λ of a surface is commonly quantified as a numerical number ranging from 0 to 1. A value of 0 signifies a surface that perfectly reflects radiation without emitting any, while a value of 1 indicates a surface that fully emits radiation. ε_λ is necessary for the estimation of the land surface temperature. Equation (7) was used to calculate the emissivity of the land surface [48]:

$$\varepsilon_\lambda = \varepsilon_{v\lambda}F_v + \varepsilon_{s\lambda}(1 - F_v) + \delta_\lambda \quad (7)$$

where $\varepsilon_{v\lambda}$ and $\varepsilon_{s\lambda}$ are the emissivity of a full vegetative surface and full soil surface, respectively. δ_λ is the surface roughness that is considered as a constant value of 0.005 [44]. Practically, Equation (7) adopted to Equation (8) as illustrates below [49]:

$$\varepsilon_\lambda \begin{cases} \varepsilon_{s\lambda}, & NDVI < NDVI_s \\ \varepsilon_{v\lambda}F_v + \varepsilon_{s\lambda}(1 - F_v) + \delta_\lambda, & NDVI_s \leq NDVI \leq NDVI_v \\ \varepsilon_{v\lambda}F_v + \delta_\lambda, & NDVI > NDVI_v \end{cases} \quad (8)$$

When the NDVI falls below 0, the pixel is considered water with an emissivity value of 0.991. NDVI values ranging from 0 to 0.2 indicate soil coverage and are assigned an emissivity value of 0.996. The range of NDVI values between 0.2 and 0.5 is classified as a combination of soil and vegetation cover, and Equation (8) is utilized to extract the emissivity. When the NDVI value exceeds 0.5 in the last scenario, it is classified as vegetation-covered and assigned a value of 0.973.

Finally, the land surface temperature (LST) is derived using Equation (9):

$$LST_k = \frac{T_B}{1 + \frac{\lambda \rho T_B}{hc} \ln \varepsilon_\lambda} \quad (9)$$

where λ is the effective wavelength, which is 10.9 mm, for Landsat 8's Band 10, ρ is Boltzmann's constant (1.38×10^{-23} J/K), h is Planck's constant (6.626×10^{-34} Js), c is the light's velocity (2.998×10^8 m/s), and ε_λ is the emissivity.

LST_k is obtained in Kelvin, then converted to Celsius using Equation (10) as depicted below:

$$LST_c = LST_k - 273.15 \quad (10)$$

where LST_c is the land surface temperature in Celsius.

QGIS Desktop version 3.22.14 (<https://www.osgeo.org/projects/qgis/> (accessed on 15–18 February 2023)) software was utilized to accomplish the remote sensing digital picture analysis, spatial analysis, and mapping.

A total of one thousand random locations was produced to encompass the whole study area. The points were utilized to gather the measurements of the NDVI, NDBI, and LST_c at their respective positions. The sampling results were exported to Minitab (<https://www.minitab.com/> (accessed on 1–3 March 2023)) to examine the correlation between the NDVI and LST_c , as well as between the NDBI and LST_c , both before and after the development of the study area.

The research has three main hypotheses, which are:

Hypothesis 1 (H1): *The Normalized Difference Vegetation Index (NDVI) has a substantial impact on the land surface temperature (LST) in the study area before and after the development.*

Hypothesis 2 (H2): *The Normalized Difference Built-Up Index (NDBI) exerts a substantial impact on the land surface temperature (LST) across the study area before and after the development.*

Hypothesis 3 (H3): *The variables NDVI and NDBI have a considerable impact on the land surface temperature change (LST_c).*

4. Results

4.1. Spatiotemporal Pattern of the NDVI and NDBI

The NDVI is a quantitative measure employed to evaluate and track the quantity of thriving vegetation inside a certain region. The spatial distribution of the NDVI over the study period is depicted in Figure 4, while Figure 5 illustrates the seasonal fluctuations of the NDVI. The NDVI values in the years 2022–2023 exhibit a decrease compared to the years 2013–2014. The average difference in the NDVI values during the years dropped by 0.028, 0.0177, 0.0235, and 0.0534, respectively. The lowest NDVI values were seen during the winters of 2014 and 2023. Conversely, the highest NDVI value was recorded during the winter of 2014, reaching 0.2667.

Researchers observed that the primary land use in the study area is characterized by medium-density residential development. Figure 6 displays the alterations in the spatial patterns of the NDBI, whereas Figure 7 illustrates the seasonal fluctuations of the NDBI before and after the development of the study area. The Normalized Difference Built-Up Index (NDBI) is a spectral index employed in remote sensing to detect and measure the extent of developed or urban regions in a given area. The highest recorded value of the NDBI occurred during the spring of 2022 at 0.0916. The mean values in the four seasons differed by 0.0002, 0.0046, 0.0042, and 0.0052, respectively, suggesting that there is no substantial variation in the NDBI over the years.

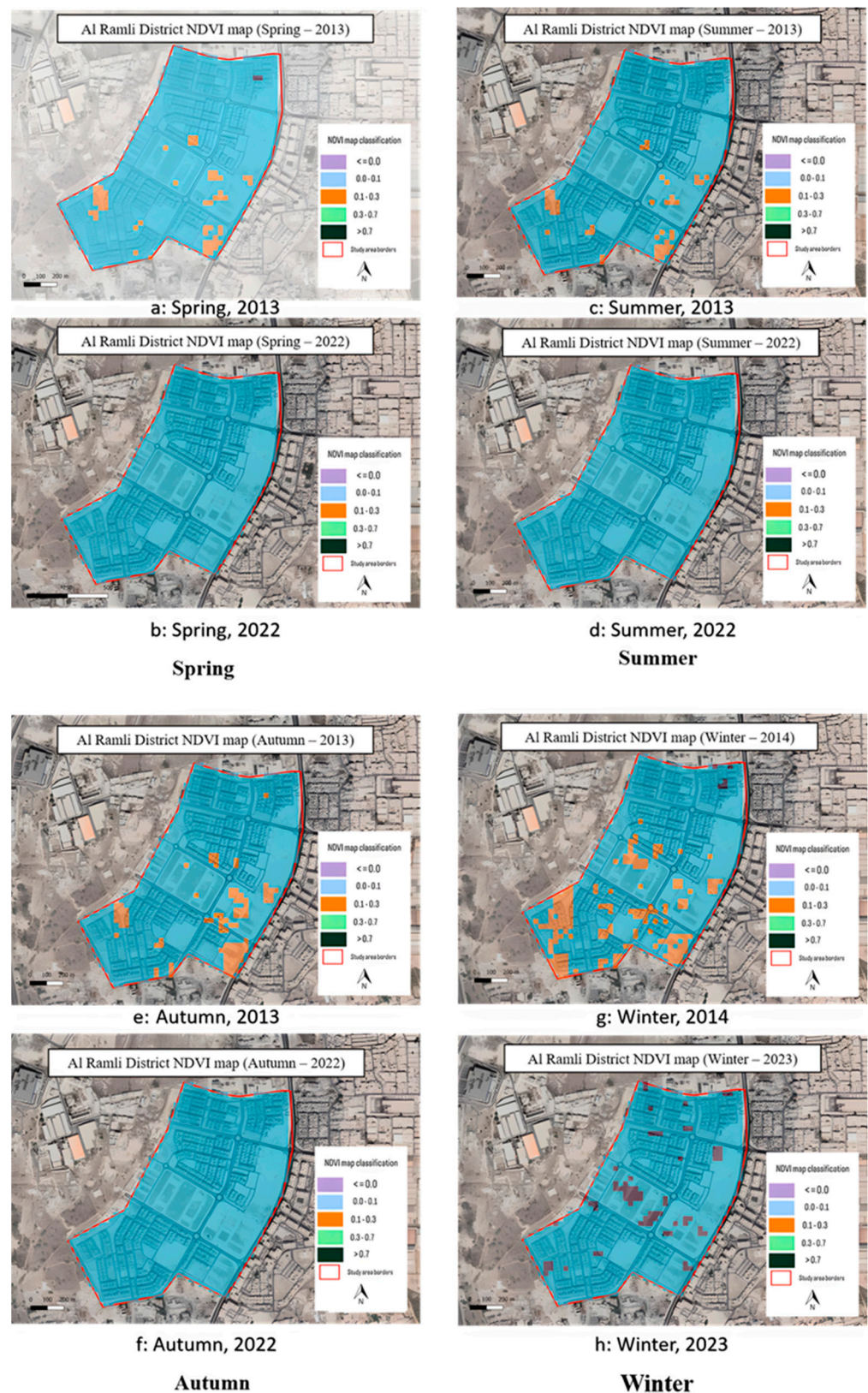


Figure 4. Spatial pattern of the NDVI over the study area at (a) Spring 2013, (b) Spring 2022, (c) Summer 2013, (d) Summer 2022, (e) Autumn 2013, (f) Autumn 2022, (g) Winter 2014, and (h) Winter 2023.

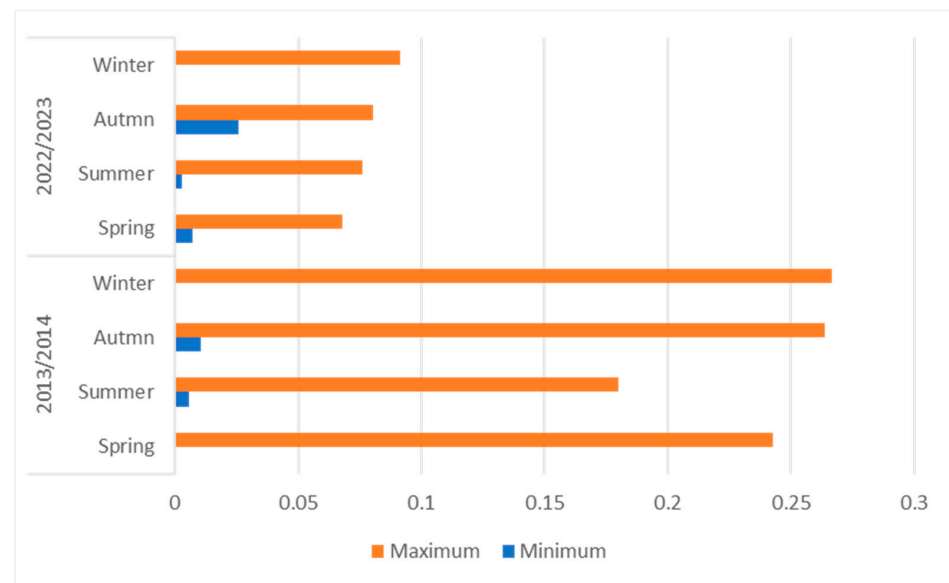


Figure 5. Seasonal variation of the land surface temperature NDVI before and after development of the study area.

4.2. Spatiotemporal Pattern of the Land Surface Temperature

The land surface temperature (LST) was derived using data from Band 10 of the Landsat 8 OLI/TIRS satellite for both the pre- and post-development periods of the study area. Figure 8 displays the categorized land surface temperature maps of the study area for the four seasons in the years 2013–2014 and 2022–2023. The LST maps identified a rise in springtime LST, with the temperature in 2013 being categorized as high. The maximum and minimum temperatures recorded were 42.8 °C and 38.2 °C, respectively. In 2022, most of the study area was categorized as having a very high LST, with some areas experiencing high LSTs. The highest recorded LST was 47.1 °C, while the lowest was 43.8 °C. In fall 2013, the temperature ranged from a maximum of 42.2 °C to a minimum of 38.1 °C, with a high LST classification. However, in 2022, the LST was significantly higher, with a maximum of 50.7 °C and a minimum of 46 °C. The LST classification remained unchanged during both the summer and winter seasons. The summer season was categorized as having an extremely high LST, whereas the winter season was categorized as having a moderate LST. The seasonal variation of the land surface temperature (LST) pre- and post-development of the study area is shown in Figure 9.

Modeling Relationships between the NDVI, NDBI, and LST

To assess, one can establish the correlation between the Normalized Difference Vegetation Index (NDVI) and land surface temperature (LST), as well as the correlation between the Normalized Difference Built-Up Index (NDBI) and LST, by doing a linear regression analysis. During the regression test, the LST will serve as the response variable (dependent variable), while the NDVI and NDBI will be used as predictor variables (independent variables). Both the NDVI and NDBI values were derived from the analysis of Landsat 8–9 OLI/TIRS C2 L2 data.

The subsequent results will delve into the variations in the LST, NDVI, and NDBI. Furthermore, it will explore the impact of the NDVI and NDBI on the LST across all four seasons within the study area.

In order to examine the association between the NDBI, NDVI, and LST in the study area, a total of 1000 randomly selected sample points were taken from the NDBI, NDVI, and LST datasets. These sample points were then utilized to conduct a regression analysis. The coefficient of determination (R^2) and Pearson correlation coefficients were obtained to assess the strength of the relationships. The linear regression models for the NDVI and LST, as well as for the NDBI and LST, are shown in Figures 10 and 11, respectively.

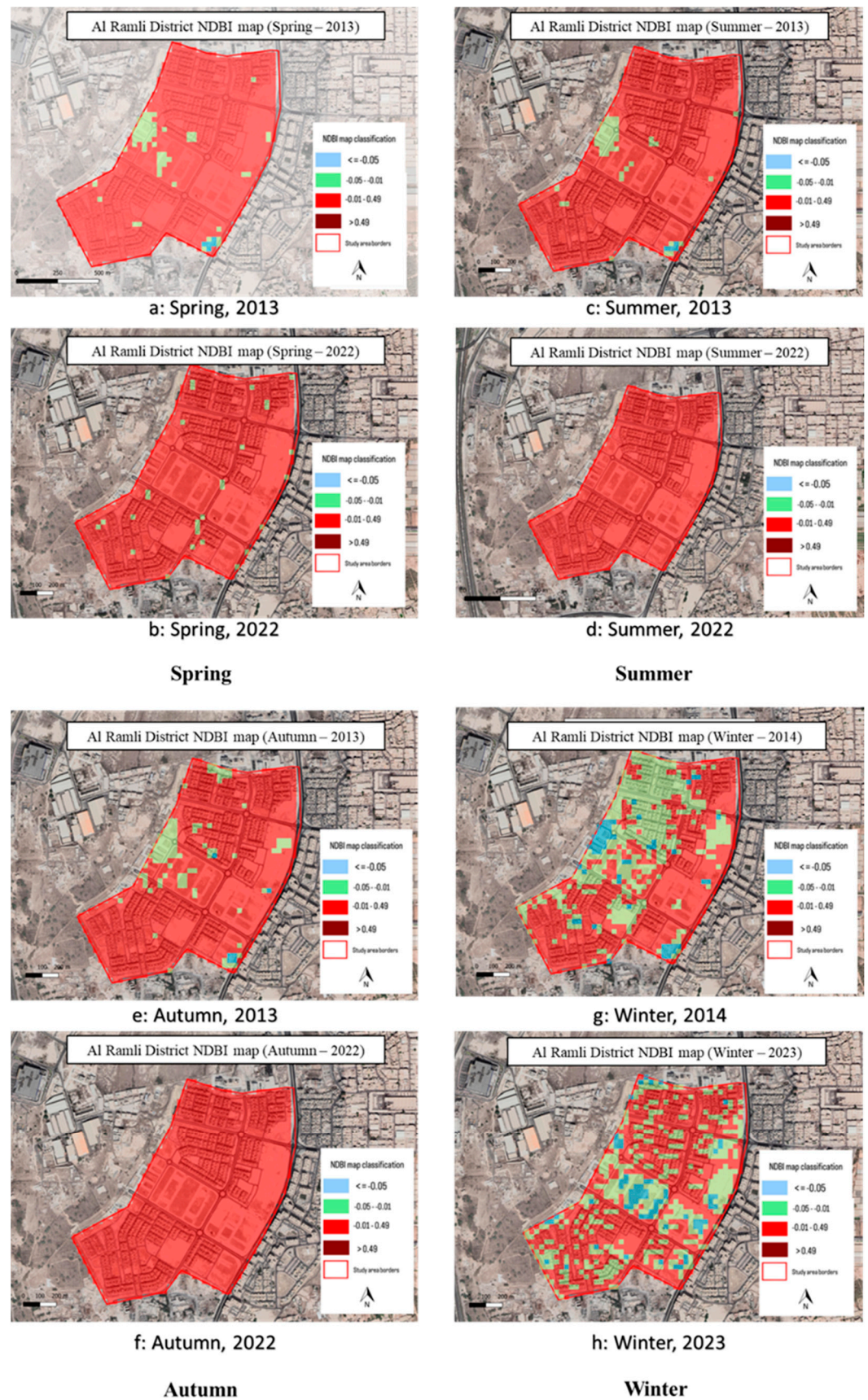


Figure 6. Spatial pattern of the NDBI over the study area at (a) Spring 2013, (b) Spring 2022, (c) Summer 2013, (d) Summer 2022, (e) Autumn 2013, (f) Autumn 2022, (g) Winter 2014, and (h) Winter 2023.

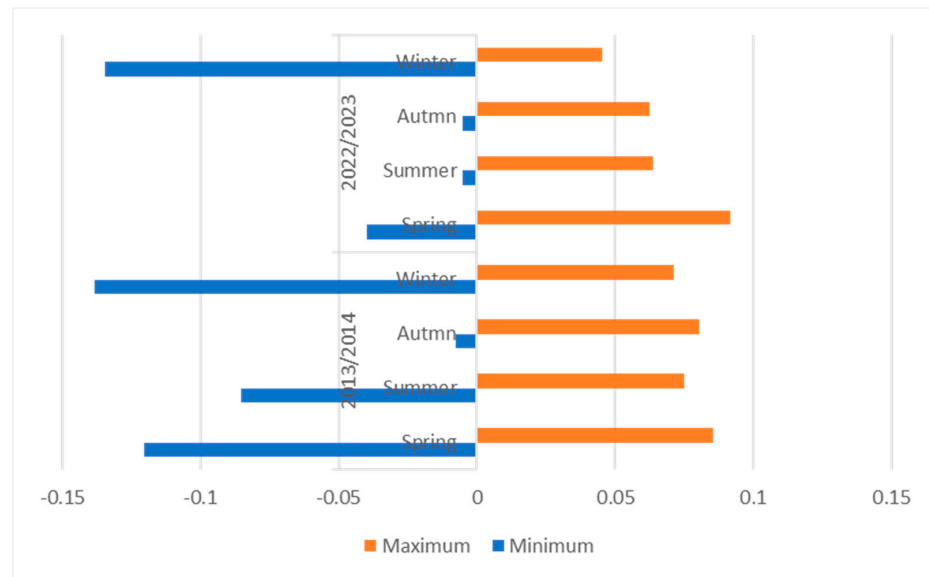


Figure 7. Seasonal variation of the land surface temperature NDBI before and after development of the study area.

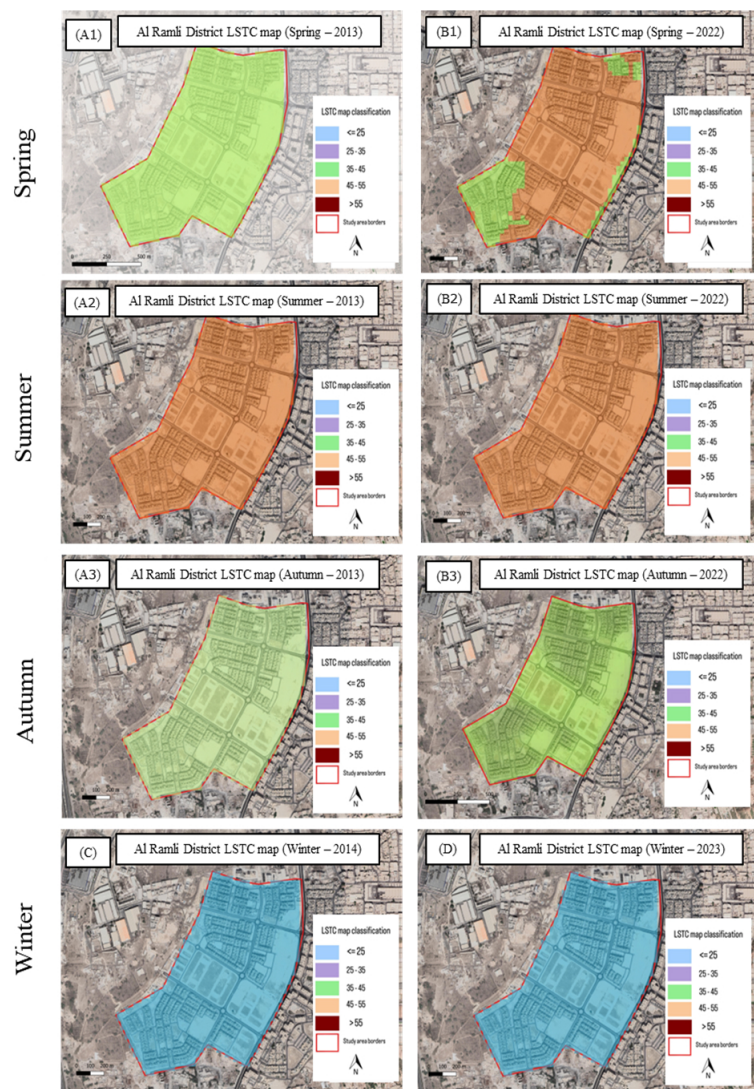


Figure 8. Spatial pattern of the LST over the study area at (A) 2013, (B) 2022, (C) 2014, (D) 2023.

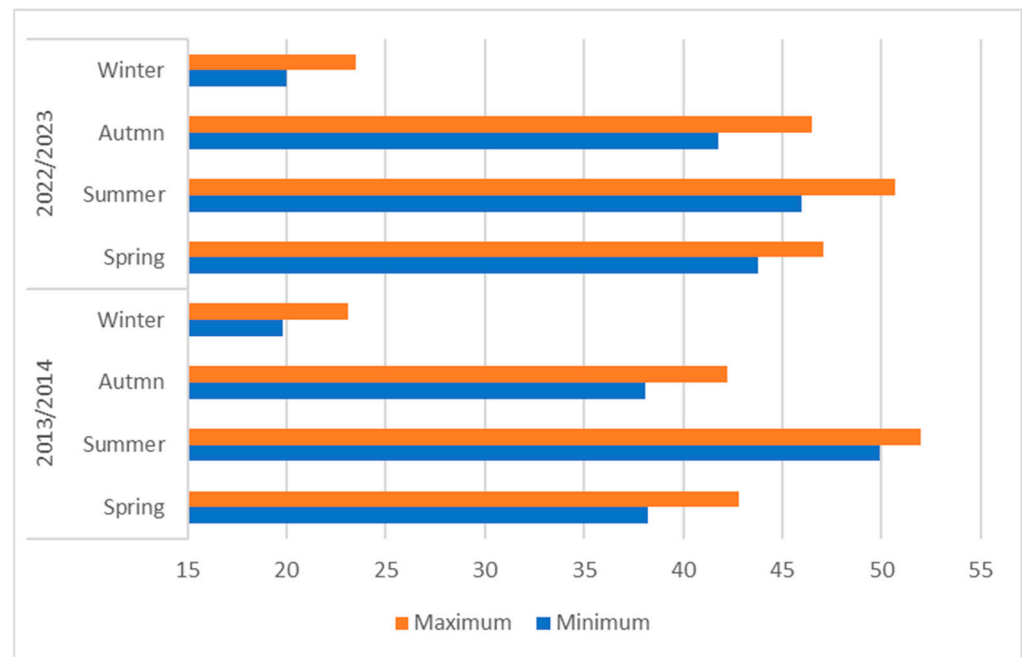


Figure 9. Seasonal variation of the land surface temperature LST before and after development of the study area.

There is a significant and consistent positive relationship between the NDBI and land surface temperature at a 95% confidence level over four seasons in the years 2013–2014 and 2022–2023. The Pearson index values for the years 2013–2014 were 0.158, 0.339, 0.360, and 0.135, respectively. For the years 2022–2023, the Pearson index values were 0.334, 0.571, 0.562, and 0.445, respectively. For each incremental rise of 0.01 in the NDBI value, the land surface temperature experienced corresponding increases of 0.05 °C, 0.08 °C, 0.08 °C, and 0.02 °C in the years 2013–2014. In the years 2022–2023, the land surface temperature climbed by 0.11 °C, 0.42 °C, 0.44 °C, and 0.11 °C, correspondingly, for the same incremental increase in the NDBI value. The correlation between the NDBI and LST indicates a consistent rise in the NDBI throughout time. The NDBI successfully identified and described the variations in the LST.

Figure 10 shows a negative association between the NDVI and LST in various seasons. For each 0.01 rise in the NDVI value, the equivalent LST in four seasons during 2013–2014 (except summer) reduced by 0.06 °C, 0.0003 °C, and 0.03 °C, respectively. In the summer season, the LST increased by 0.0025 °C. From 2022 to 2023, the LST was projected to rise by 0.18 °C, 0.61 °C, and 0.64 °C, respectively, and experience a decrease of 0.01 °C during the winter season. Hence, the NDVI exhibited sensitivity towards variations in the LST, and any disagreement in the NDVI could potentially lead to a modification in the LST. The NDVI and LST exhibited a negative correlation during the spring, fall, and winter seasons of 2013–2014. The Pearson coefficient, calculated at a 95% level of confidence, was determined to be -0.18 , -0.016 , and -0.192 , respectively. In the summer, there was a positive correlation between the variables, as indicated by a Pearson value of 0.01. In contrast, over the period of 2022–2023, there was a positive correlation between the NDBI and LST in the spring, summer, and fall as shown in Figure 11, this correlation was statistically significant at a 95% confidence level, with Pearson coefficients of 0.310, 0.496, and 0.512, respectively. The association exhibited a negative correlation throughout the winter season, with a Pearson coefficient of -0.025 . However, despite the shifting seasons, the correlation between the NDVI and LST was not consistent, which was the same as Chen [50].

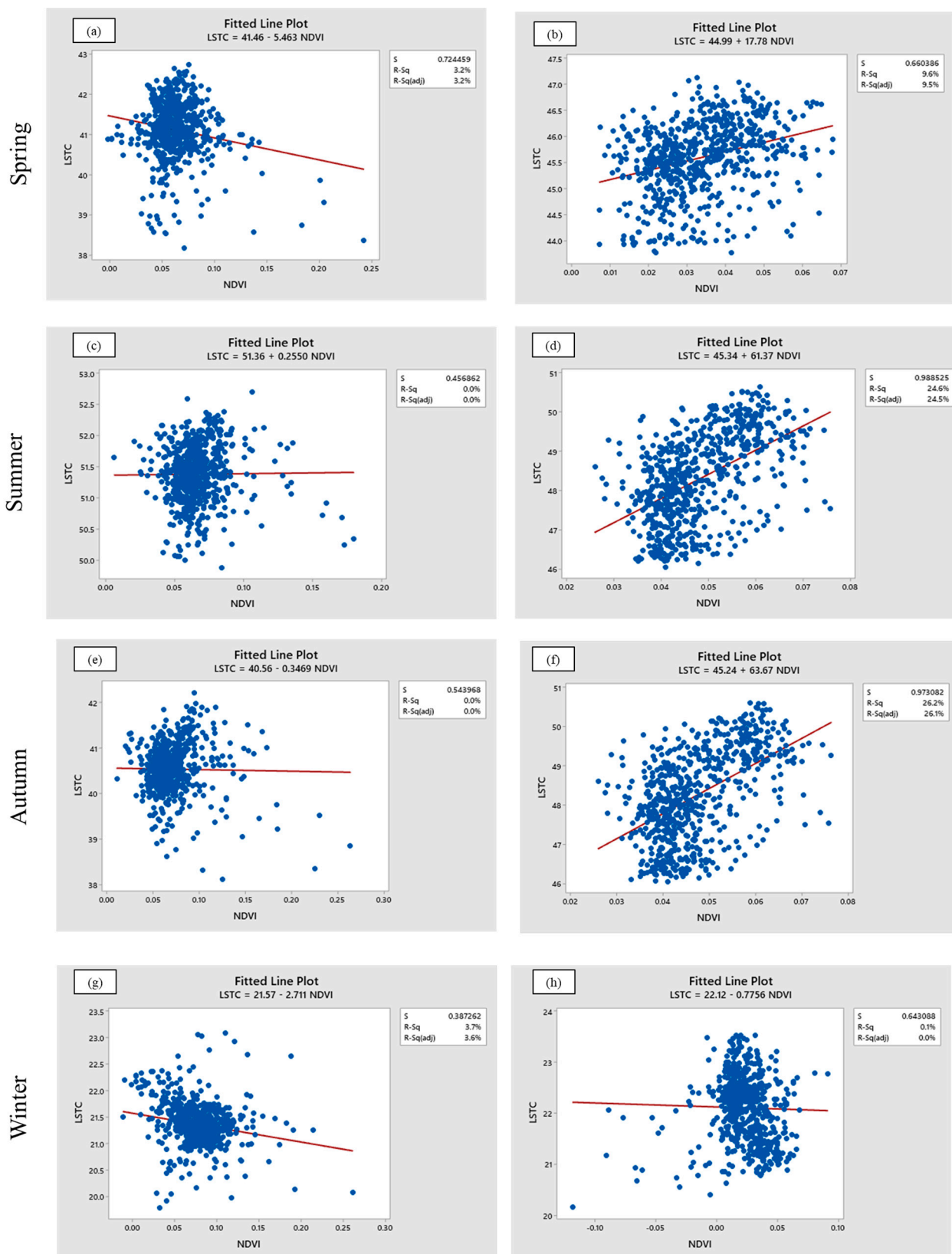


Figure 10. Regression models for the NDVI and LST at (a) Spring 2013, (b) Spring 2022, (c) Summer 2013, (d) Summer 2022, (e) Autumn 2013, (f) Autumn 2022, (g) Winter 2014, and (h) Winter 2023.



Figure 11. Regression models for the NDBI and LST at (a) Spring 2013, (b) Spring 2022, (c) Summer 2013, (d) Summer 2022, (e) Autumn 2013, (f) Autumn 2022, (g) Winter 2014, and (h) Winter 2023.

During the year 2013–2014, there was a negative connection between the NDBI and NDVI in the seasons of the spring, summer, and winter. The Pearson index values for these seasons were -0.16 , -0.076 , and -0.147 , respectively. However, in the autumn season, there was a positive correlation, with a Pearson index value of 0.021 . In addition, throughout the period of 2022–2023, there was a strong positive association seen between the NDBI and NDVI in all four seasons. The Pearson index values were 0.286 , 0.663 , 0.62 , and 0.24 . The correlation between the NDVI and land utilization for urban construction was evident, as it accurately depicted the changes that occurred over time.

5. Discussion

As explained earlier, the Kingdom of Bahrain is located in the Arabian Gulf on the peninsula's east coast. Despite being an island country with a limited land area, it is threatened by global environmental issues such as the global warming phenomenon, sea level rise, etc. At the same time, it has characteristics similar to those of other countries in the same area; given the similarities in geographical factors and proximity to other regions on the east coast of the Arabian Peninsula, the results of this research conducted in Bahrain can provide insights and knowledge that may apply to different regions in the area. Therefore, the researchers took it as an excellent example of a pilot study.

In another words, the results of a study conducted in Bahrain can potentially be generalized to other regions on the east coast of the Arabian Peninsula. Given the similarities in geographical characteristics and proximity to other regions on the east coast of the Arabian Peninsula, the results of a study conducted in Bahrain can provide insights and knowledge that may be applicable to other regions in the area. Although limited-scale studies may not always allow for a direct generalization of results to other regions, they offer numerous benefits in terms of the depth of understanding, local relevance, baseline data generation, and informing broader research and action agendas. However, it is important to consider the specific context and characteristics of each region when generalizing the findings of a study.

Using Bahrain as an example of a city that has seen a population increase and urban expansion, the tendency of the study area's population increase in conjunction with the LST will persist in the Gulf Cooperation Council (GCC). This could harm the urban runoff pattern, climate conditions, and the livable environment. Before any additional alterations to its unorganized constructed surroundings, the city necessitates the focus of urban planners and policymakers to prevent any distortion in LST patterns. Therefore, under the umbrella of sustainability, the research took Al Ramila's residential project in Bahrain as an example of a government residential project in the Gulf Cooperation Council (GCC) to study the possibility of UHIs and to investigate the influence of land use changes in a small-scale urban landscape, putting the UHI under the spotlight to enhance environmental construction practices in the region. As explained earlier in the introduction, referring to sustainability, the topic is whether the ongoing residential projects within the rapid urbanization projects are ecologically sustainable and ensure quality of life. By matching Bahrain's 2023 strategy and goals and the residential projects, according to the discussed cases, the research strives to study the compatibility between such projects with the Sustainable Development 2030 Agenda adopted by the United Nations and its implementation in the GCC [11]. Moreover, the authority works hard to create sustainable local development consistent with the comprehensive strategic plan for Bahrain 2023 [12].

As understood from the background of the study area, the Al Ramila suburb had a shortage of vegetation for a long time due to its function as a construction dumping area, which negatively affected its land characteristics. These issues were impacted by the readings of the temperature of the land cover before and after the construction of the residential projects. This point added significance to studying such a project. From another other point of view, according to the expectations of the increasing rate of global climate change and the increase in land surface temperature (LST) and the rising rate of global climate change, this research studied the projected increase in land surface temperature

(LST) in general and in hot climates, including the countries of the Gulf Cooperation Council (GCC). The research briefly discussed the massive change in land use and its cover due to the high demand for urban land to accommodate additional residential developments accompanying the surge in population growth spanning from 2013 to 2023, which was undertaken to achieve this goal and match with the 2023 strategies. The point of discussion in this research is seriously significant in such a field to discover the phenomena occurring in urban heat islands in such metropolitan areas. Moreover, discussing the research results will enhance the quality of the urban environment and improve the social conditions in these residential areas. Furthermore, economically, it has an impact on decreasing the power consumption and the cost of residents' living expenses, as well as reducing the economic forces of the GCC.

A comprehensive analysis was performed pre- and post-construction development, approaching all seasons of the year to study the UHI intensity, along with the investigation of LST relationships with both the NDBI and NDVI. Hypothesis 1 was partially rejected, while both Hypotheses 2 and 3 were accepted.

Wrapping up, the outcomes of the discussion of the research's hypotheses are:

Hypothesis 1 (H1): *is partially rejected, because the correlation between the LST and NDVI was not stable; although the vegetation index was sensitive to LST fluctuations, the NDVI did not reflect LST stably.*

Hypothesis 2 (H2): *H2 is accepted, because the NDBI and LST correspondence was stable; hence, the NDBI can reflect LST variations stably.*

Hypothesis 3 (H3): *is accepted, as the statical results support the hypothesis' validity.*

The results showed that changes in the land cover from its natural habitat and soil into manufactured materials that capture and release heat as concrete and asphalt contributed to forming UHIs by raising temperatures; this was clearly displayed in the NDBI and LST relationship. Meanwhile, the NDVI and LST relation showed the absence of stability by showing positive and negative correlations over the seasons.

This study employed Landsat 8 OLI/TIRS images to examine the correlation between urban development and temperature fluctuations using the Normalized Difference Vegetation Index (NDVI), Normalized Difference Built-Up Index (NDBI), and land surface temperature (LST) as the primary indicators. The study area was in the Kingdom of Bahrain, and the analysis was conducted from 2013 to 2023. The urban growth in the study area was assessed based on the results of the NDBI. Urban expansion has created additional residential space, albeit at the natural environment's expense. The LST exhibited significant rises throughout the summer months following urban growth in contrast to the period before development. The mean LST increased from 41.1 °C to 45.6 °C during the spring and from 40.5 °C to 44.2 °C during the autumn following the implementation of urban growth in the studied area. In this overall pattern, the study area's land surface temperature (LST) experienced a more noticeable increase.

Furthermore, our investigation into the relationship between the Normalized Difference Built-Up Index (NDBI) and land surface temperature (LST) yielded insightful findings that underscored the effectiveness of the NDBI in describing LST dynamics within the studied small-scale urban development projects in the Gulf Cooperation Council (GCC) region. A notable positive correlation was observed between the NDBI and LST, revealing that, as the NDBI values increased, there was a corresponding elevation in the LST. This positive association underscores the potential of the NDBI as a reliable indicator for gauging thermal patterns in urban environments, particularly in the context of small-scale developments. Conversely, our analysis also revealed a negative correlation between the Normalized Difference Vegetation Index (NDVI) and LST. Higher NDVI values were associated with a lower LST, highlighting the cooling effect of vegetation within the urban landscape. However, it is essential to note that the relationship between the NDVI and LST

exhibited a degree of instability. Despite the generally negative correlation, the NDVI–LST dynamic proved less consistent, suggesting that the NDVI may not consistently reflect LST variations in small-scale urban development areas.

Also, since the NDVI and LST relationship was not stable, it is suggested to consider different approaches for monitoring their interactions. Since this study was conducted pre- and post-construction of the project, a study is recommended that compares UHIs between two different periods after the construction to evaluate whether the construction was environmentally friendly or not to check such projects with the national plan in achieving sustainability in the residential projects, as well as matching with the 2023 strategies to enhance the quality of the urban environment and improve social interactions within the residential areas.

The study's results matched the findings of Elghoneimy and Mohammed 2019 [51]. It evaluated the relations between the spectral indices of impervious materials and vegetation on the one hand and the thermal settings on the other; it displays the significance of considering the quantity of vegetation land cover in residential projects in the Gulf Countries. Consequently, it will impact the local economy in the GCC. These results are alarming because of the possible negative impacts of such residential projects with their conditions upon the local environment at the micro- and macroclimatic, economic, ecological, and urban levels.

Finally, the residential projects are running in many locations and rapidly increasing. Unfortunately, using the same construction performance will lead to high expectations of creating non-sustainable projects and will lead to UHIs, too. It means low social quality, overloading for the economy due to high consumption for air conditioning issues, as well as negative impacts upon the environment, with various problems.

Consequently, the overall urban quality in such project zones will deteriorate. It should be noted that the subject of UHIs alerts the environment at different levels, and these projects are scattered in other locations and various urban circumstances. Therefore, there is a need for further studies to avoid the negative impacts that may result due to such a project.

The research limitation was in a specific construction phase of a governmental project with certain characteristics and borders to enable comprehensive analyses due to the time factors and the limited financial resources, as the research had a minimal source. Therefore, future research should cover similar projects in different areas of the GCC based on the significance of controlling the reasons for occurring UHIs to prevent the possible negative impacts of creating UHIs in other regions of the city's urban spaces.

6. Conclusions

In the context of global climate change, the projected increase in land surface temperature (LST) worldwide, particularly in the GCC, amplifies its negative impacts on the quality of life in the new residential projects. This concerns local authorities in the GCC countries, which have hot climates, including Bahrain in the Gulf Cooperation Council (GCC). As examined in the research, with a surge in population growth, there is a high demand for residential projects, which forces the authorities to plan to construct a large number of residential projects on the governmental side, as well as encouraging the private sector from the other side to invest in such projects. Consequently, it has led to a heightened demand for land and many influences on land use changes.

Using multispectral remote sensing data with a moderate spatial resolution, specifically Landsat 8 OLI/TIRS, this study demonstrated a significant potential for predicting the variations in thermal settings in newly urbanized areas. This would enable new urban development projects to consider the possibility of variations and improve their projects' resilience. Therefore, increased spatial resolution remote sensing data may be necessary in order to guarantee environmentally responsible and accurate predictions for such development initiatives, which will be our objective in future works. The evaluation of the relations between the spectral indices of impervious materials and vegetation, on the one hand,

and the thermal settings, on the other hand, as presented in this study, demonstrated the significance of considering the amount of vegetation land cover in new urban communities in the Gulf's countries, particularly in the Kingdom of Bahrain, which agrees with the findings of Elghoneimy and Mohammed 2019 [51].

These findings empirically support the idea that small-scale residential developments contribute to notable LST increases, primarily due to expanded impervious surfaces. These insights can potentially inform localized adaptation strategies for residential development projects, crucial for managing the impacts of rising land surface temperatures. Therefore, it is of the utmost importance to ensure that the study outcomes are influenced by the environmental conditions of the local area. Following that, the framework presented in this research can be effectively utilized in comparable surroundings and conditions, with some limitations considered, to evaluate and forecast the future variations of urban thermal settings. In the same concern, from an urban planning point of view, the different strategies of the residential projects focused on sustainable projects matching with the 2023 strategies, which had to take the results of this research seriously in studying possible solutions to reduce the negative impacts of the current projects' conditions, which create urban heat islands in such urban areas. Moreover, from an environmental point of view, using these research results will not only enhance the quality of the urban environment but also improve the social interactions within the open spaces in the residential areas of the urban context. Furthermore, economically, it will lead to modifying the conditions and characteristics of such residential projects and decrease power consumption. Consequently, it will lower the cost of residents' living expenses and reduce the economic forces in the GCC.

Finally, the study's results are alarming because of the possible negative impacts of such residential projects with their conditions upon the local environment at the micro- and macroclimatic, economic, ecological, and urban levels.

Author Contributions: M.A. did the methodology, data collection, site study, and data curation as part of her Master's thesis; W.M. supervised the methodology, paper validation, and software; M.A.A. administered the project, secured funding, and reviewed the paper broadly; E.M. did the formal analysis and the visualization, N.A.A. contributed to the project administration and review; and I.E. focused on conceptualization, writing—review and editing, and supervision of the research progress. All authors have read and agreed to the published version of the manuscript.

Funding: The publication of the work was supported and funded by the Deanship of Scientific Research at Imam Mohammad Ibn Saud Islamic University (IMSIU) (grant number IMSIU-RG23116).

Institutional Review Board Statement: Not applicable.

Informed Consent Statement: Not applicable.

Data Availability Statement: The research data are found in the research manuscript.

Conflicts of Interest: The authors declare no conflicts of interest.

References

1. Das, A.; Saha, P.; Dasgupta, R.; Inacio, M.; Das, M.; Pereira, P. How Do the Dynamics of Urbanization Affect the Thermal Environment? A Case from an Urban Agglomeration in Lower Gangetic Plain (India). *Sustainability* **2024**, *16*, 1147. [\[CrossRef\]](#)
2. Yang, S.; Wang, L.; Stathopoulos, T.; Marey, A. Urban microclimate and its impact on built environment: A review. *Build. Environ.* **2023**, *238*, 110334. [\[CrossRef\]](#)
3. Pan, L.; Yang, C.; Han, J.; Yan, F.; Ju, A.; Kui, T. Comparing the Evolution of Land Surface Temperature and Driving Factors between Three Different Urban Agglomerations in China. *Sustainability* **2024**, *16*, 486. [\[CrossRef\]](#)
4. Ashwini, K.; Sil, B.S. Impacts of Land Use and Land Cover Changes on Land Surface Temperature over Cachar Region, Northeast India—A Case Study. *Sustainability* **2022**, *14*, 14087. [\[CrossRef\]](#)
5. Przeździecki, K.; Zawadzki, J. Impact of the Variability of Vegetation, Soil Moisture, and Building Density between City Districts on Land Surface Temperature, Warsaw, Poland. *Sustainability* **2023**, *15*, 1274. [\[CrossRef\]](#)
6. Seletković, A.; Kičić, M.; Ančić, M.; Kolić, J.; Pernar, R. The Urban Heat Island Analysis for the City of Zagreb in the Period 2013–2022 Utilizing Landsat 8 Satellite Imagery. *Sustainability* **2023**, *15*, 3963. [\[CrossRef\]](#)

7. Jamei, Y.; Seyedmahmoudian, M.; Jamei, E.; Horan, B.; Mekhilef, S.; Stojcevski, A. Investigating the Relationship between Land Use/Land Cover Change and Land Surface Temperature Using Google Earth Engine; Case Study: Melbourne, Australia. *Sustainability* **2022**, *14*, 14868. [[CrossRef](#)]
8. Wu, Z.; Zhang, X.; Ma, P.; Kwan, M.-P.; Liu, Y. How Did Urban Environmental Characteristics Influence Land Surface Temperature in Hong Kong from 2017 to 2022? Evidence from Remote Sensing and Land Use Data. *Sustainability* **2023**, *15*, 15511. [[CrossRef](#)]
9. Naughton, J.; McDonald, W. Evaluating the Variability of Urban Land Surface Temperatures Using Drone Observations. *Remote Sens.* **2019**, *11*, 1722. [[CrossRef](#)]
10. Gao, S.; Zhan, Q.; Yang, C.; Liu, H. The Diversified Impacts of Urban Morphology on Land Surface Temperature among Urban Functional Zones. *Int. J. Environ. Res. Public Health* **2020**, *17*, 9578. [[CrossRef](#)]
11. Bahrain Center for Strategic, International and Energy Studies. *Bahrain Human Development Report 2018—Pathways to Sustainable Economic Growth in Bahrain*; Bahrain Center for Strategic, International and Energy Studies: Riffa, Bahrain, 2018.
12. UN-DESAPD. *World Urbanization Prospects: The 2018 Revision*; United Nations, Department of Economic and Social Affairs, Population Division (UN-DESAPD): New York, NY, USA, 2019.
13. Eie, Q.; Xu, J. Understanding the effects of the impervious surfaces pattern on land surface temperature in an urban area. *Front. Earth Sci.* **2015**, *9*, 276–285.
14. Population and Demographics; Ministry of Information: Bahrain, 2023. Available online: <https://www.mia.gov.bh/kingdom-of-bahrain/population-and-demographics/?lang=en> (accessed on 28 February 2023).
15. Bahrain Demographics; United Nations, Department of Economic and Social Affairs, Population Division. World Population Prospects; (Medium-Fertility Variant). [Worldometers.info](https://www.worldometers.info/world-population/bahrain-population/); Bahrain Population. 2024. Available online: <https://www.worldometers.info/world-population/bahrain-population/> (accessed on 28 February 2023).
16. Loridan, T.; Grimmond, C.S.B. Characterization of Energy Flux Partitioning in Urban Environments: Links with Surface Seasonal Properties. *J. Appl. Meteorol. Climatol.* **2012**, *51*, 219–241. [[CrossRef](#)]
17. Kotthaus, S.; Grimmond, C.S.B. Energy Exchange in a Dense Urban Environment—Part I: Temporal Variability of Long-Term Observations in Central London. *Urban Clim.* **2014**, *10*, 261–280. [[CrossRef](#)]
18. Kotthaus, S.; Grimmond, C.S.B. Energy Exchange in a Dense Urban Environment—Part II: Impact of Spatial Heterogeneity of the Surface. *Urban Clim.* **2014**, *10*, 281–307. [[CrossRef](#)]
19. Ghosh, S.; Chatterjee, N.D.; Dinda, S. Relation between Urban Biophysical Composition and Dynamics of Land Surface Temperature in the Kolkata Metropolitan Area: A GIS and Statistical Based Analysis for Sustainable Planning. *Model. Earth Syst. Environ.* **2019**, *5*, 307–329. [[CrossRef](#)]
20. Xiang, Y.; Huang, C.; Huang, X.; Zhou, Z.; Wang, X. Seasonal Variations of the Dominant Factors for Spatial Heterogeneity and Time Inconsistency of Land Surface Temperature in an Urban Agglomeration of Central China. *Sustain. Cities Soc.* **2021**, *75*, 103285. [[CrossRef](#)]
21. Wang, Y.; Zhan, Q.; Ouyang, W. Impact of Urban Climate Landscape Patterns on Land Surface Temperature in Wuhan, China. *Sustainability* **2017**, *9*, 1700. [[CrossRef](#)]
22. Bian, T.; Ren, G.; Yue, Y. Effect of Urbanization on Land-Surface Temperature at an Urban Climate Station in North China. *Bound.-Layer Meteorol.* **2017**, *165*, 553–567. [[CrossRef](#)]
23. Li, Z.; Wu, H.; Duan, S.; Zhao, W.; Ren, H.; Liu, X.; Leng, P.; Tang, R.; Ye, X.; Zhu, J.; et al. Satellite Remote Sensing of Global Land Surface Temperature: Definition, Methods, Products, and Applications. *Rev. Geophys.* **2023**, *61*, e2022RG000777. [[CrossRef](#)]
24. Nega, W.; Balew, A. The Relationship between Land Use Land Cover and Land Surface Temperature Using Remote Sensing: Systematic Reviews of Studies Globally over the Past 5 Years. *Environ. Sci. Pollut. Res.* **2022**, *29*, 42493–42508. [[CrossRef](#)]
25. Reiners, P.; Sobrino, J.; Kuenzer, C. Satellite-Derived Land Surface Temperature Dynamics in the Context of Global Change—A Review. *Remote Sens.* **2023**, *15*, 1857. [[CrossRef](#)]
26. Ndossi, M.; Avdan, U. Inversion of Land Surface Temperature (LST) Using Terra ASTER Data: A Comparison of Three Algorithms. *Remote Sens.* **2016**, *8*, 993. [[CrossRef](#)]
27. Cristóbal, J.; Jiménez-Muñoz, J.; Prakash, A.; Mattar, C.; Skoković, D.; Sobrino, J. An Improved Single-Channel Method to Retrieve Land Surface Temperature from the Landsat-8 Thermal Band. *Remote Sens.* **2018**, *10*, 431. [[CrossRef](#)]
28. Choudhury, D.; Das, K.; Das, A. Assessment of Land Use Land Cover Changes and Its Impact on Variations of Land Surface Temperature in Asansol-Durgapur Development Region. *Egypt. J. Remote Sens. Space Sci.* **2019**, *22*, 203–218. [[CrossRef](#)]
29. Mumtaz, F.; Tao, Y.; De Leeuw, G.; Zhao, L.; Fan, C.; Elnashar, A.; Bashir, B.; Wang, G.; Li, L.; Naeem, S.; et al. Modeling Spatio-Temporal Land Transformation and Its Associated Impacts on Land Surface Temperature (LST). *Remote Sens.* **2020**, *12*, 2987. [[CrossRef](#)]
30. Wang, R.; Hou, H.; Murayama, Y.; Derdouri, A. Spatiotemporal Analysis of Land Use/Cover Patterns and Their Relationship with Land Surface Temperature in Nanjing, China. *Remote Sens.* **2020**, *12*, 440. [[CrossRef](#)]
31. Dutta, D.; Rahman, A.; Paul, S.K.; Kundu, A. Impervious Surface Growth and Its Inter-Relationship with Vegetation Cover and Land Surface Temperature in Peri-Urban Areas of Delhi. *Urban Clim.* **2021**, *37*, 100799. [[CrossRef](#)]
32. Zhang, Y.; Balzter, H.; Li, Y. Influence of Impervious Surface Area and Fractional Vegetation Cover on Seasonal Urban Surface Heating/Cooling Rates. *Remote Sens.* **2021**, *13*, 1263. [[CrossRef](#)]
33. Yang, C.; Yan, F.; Lei, X.; Ding, X.; Zheng, Y.; Liu, L.; Zhang, S. Investigating Seasonal Effects of Dominant Driving Factors on Urban Land Surface Temperature in a Snow-Climate City in China. *Remote Sens.* **2020**, *12*, 3006. [[CrossRef](#)]

34. Tang, J.; Di, L.; Xiao, J.; Lu, D.; Zhou, Y. Impacts of Land Use and Socioeconomic Patterns on Urban Heat Island. *Int. J. Remote Sens.* **2017**, *38*, 3445–3465. [[CrossRef](#)]
35. Dissanayake, D.; Morimoto, T.; Murayama, Y.; Ranagalage, M.; Handayani, H.H. Impact of Urban Surface Characteristics and Socio-Economic Variables on the Spatial Variation of Land Surface Temperature in Lagos City, Nigeria. *Sustainability* **2018**, *11*, 25. [[CrossRef](#)]
36. Elagib, N.A.; Addin Abdu, A.S. Climate variability and aridity in Bahrain. *J. Arid. Environ.* **1997**, *36*, 405–419. [[CrossRef](#)]
37. Ihlen, V. *Landsat 8 (L8) Data Users Handbook*; U.S. Geological Survey: Sioux Falls, SD, USA, 2019.
38. Chavez, P.S. An Improved Dark-Object Subtraction Technique for Atmospheric Scattering Correction of Multispectral Data. *Remote Sens. Environ.* **1988**, *24*, 459–479. [[CrossRef](#)]
39. Glenn, D.M.; Tabb, A. Evaluation of Five Methods to Measure Normalized Difference Vegetation Index (NDVI) in Apple and Citrus. *Int. J. Fruit Sci.* **2019**, *19*, 191–210. [[CrossRef](#)]
40. Huang, S.; Tang, L.; Hupy, J.P.; Wang, Y.; Shao, G. A Commentary Review on the Use of Normalized Difference Vegetation Index (NDVI) in the Era of Popular Remote Sensing. *J. For. Res.* **2021**, *32*, 1–6. [[CrossRef](#)]
41. Zha, Y.; Gao, J.; Ni, S. Use of Normalized Difference Built-up Index in Automatically Mapping Urban Areas from TM Imagery. *Int. J. Remote Sens.* **2003**, *24*, 583–594. [[CrossRef](#)]
42. Bhatti, S.S.; Tripathi, N.K. Built-up Area Extraction Using Landsat 8 OLI Imagery. *GIScience Remote Sens.* **2014**, *51*, 445–467. [[CrossRef](#)]
43. Yu, X.; Guo, X.; Wu, Z. Land Surface Temperature Retrieval from Landsat 8 TIRS—Comparison between Radiative Transfer Equation-Based Method, Split Window Algorithm and Single Channel Method. *Remote Sens.* **2014**, *6*, 9829–9852. [[CrossRef](#)]
44. Vanhellemont, Q. Combined Land Surface Emissivity and Temperature Estimation from Landsat 8 OLI and TIRS. *ISPRS J. Photogramm. Remote Sens.* **2020**, *166*, 390–402. [[CrossRef](#)]
45. Tan, K.; Liao, Z.; Du, P.; Wu, L. Land Surface Temperature Retrieval from Landsat 8 Data and Validation with Geosensor Network. *Front. Earth Sci.* **2017**, *11*, 20–34. [[CrossRef](#)]
46. Zhang, X.; Liao, C.; Li, J.; Sun, Q. Fractional Vegetation Cover Estimation in Arid and Semi-Arid Environments Using HJ-1 Satellite Hyperspectral Data. *Int. J. Appl. Earth Obs. Geoinf.* **2013**, *21*, 506–512. [[CrossRef](#)]
47. Sobrino, J.A.; Raissouni, N. Toward Remote Sensing Methods for Land Cover Dynamic Monitoring: Application to Morocco. *Int. J. Remote Sens.* **2000**, *21*, 353–366. [[CrossRef](#)]
48. Guha, S.; Govil, H.; Dey, A.; Gill, N. Analytical Study of Land Surface Temperature with NDVI and NDBI Using Landsat 8 OLI and TIRS Data in Florence and Naples City, Italy. *Eur. J. Remote Sens.* **2018**, *51*, 667–678. [[CrossRef](#)]
49. Wang, F.; Qin, Z.; Song, C.; Tu, L.; Karnieli, A.; Zhao, S. An Improved Mono-Window Algorithm for Land Surface Temperature Retrieval from Landsat 8 Thermal Infrared Sensor Data. *Remote Sens.* **2015**, *7*, 4268–4289. [[CrossRef](#)]
50. Chen, L.; Li, M.; Huang, F.; Xu, S. Relationships of LST to NDBI and NDVI in Wuhan City based on Landsat ETM+ image. In Proceedings of the 2013 6th International Congress on Image and Signal Processing (CISP), Hangzhou, China, 16–18 December 2013; pp. 840–845.
51. Elghonaimy, I.; Mohammed, W. Urban Heat Island in Bahrain: Urban Perspective. *Buildings* **2019**, *9*, 96. [[CrossRef](#)]

Disclaimer/Publisher’s Note: The statements, opinions and data contained in all publications are solely those of the individual author(s) and contributor(s) and not of MDPI and/or the editor(s). MDPI and/or the editor(s) disclaim responsibility for any injury to people or property resulting from any ideas, methods, instructions or products referred to in the content.